Journal of Physics: Condensed Matter

PAPER • **OPEN ACCESS**

Topological description of the solidification of undercooled fluids and the temperature dependence of the thermal conductivity of crystalline and glassy solids above approximately 50 K

To cite this article: Caroline S Gorham and David E Laughlin 2019 *J. Phys.: Condens. Matter* **31** 105701

OPEN ACCESS
IOP Publishing
Journal of Physics: Condensed Matter
J. Phys.: Condens. Matter **31** (2019) 105701 (14pp)
https://doi.org/10.1088/1361-648X/aaf8d2

Topological description of the solidification of undercooled fluids and the temperature dependence of the thermal conductivity of crystalline and glassy solids above approximately 50 K

Caroline S Gorham and David E Laughlin

Department of Materials Science and Engineering, Carnegie Mellon University, Pittsburgh, PA 15213, United States of America

E-mail: caroling@cmu.edu and laughlin@cmu.edu

Received 20 September 2018, revised 4 December 2018
Accepted for publication 17 December 2018
Published 23 January 2019

Abstract

Topological origins of the thermal transport properties of crystalline and non-crystalline solid states are considered herein, by the adoption of a quaternion orientational order parameter to describe solidification. Global orientational order, achieved by spontaneous symmetry breaking, is prevented at finite temperatures for systems that exist in restricted dimensions (Mermin–Wagner theorem). Just as complex ordered systems exist in restricted dimensions in 2D and 1D, owing to the dimensionality of the order parameter, quaternion ordered systems in 4D and 3D exist in restricted dimensions. Just below the melting temperature, misorientational fluctuations in the form of spontaneously generated topological defects prevent the development of the solid state. Such solidifying systems are well-described using O(4) quantum rotor models, and a defect-driven Berezinskii–Kosterlitz–Thouless transition is anticipated to separate an undercooled fluid from a crystalline solid state. In restricted dimensions, in addition to orientationally-ordered ground states, orientationally-disordered ground states may be realized by tuning a non-thermal parameter in the relevant O(n) quantum rotor model Hamiltonian. Thus, glassy solid states are anticipated to exist as distinct ground states of O(4) quantum rotor models. Within this topological framework for solidification, the finite Kauzmann temperature marks a first-order transition between crystalline and glassy solid states at a 'self-dual' critical point that belongs to O(4) quantum rotor models. This transition is a higher-dimensional analogue to the quantum phase transition that belongs to O(2) Josephson junction arrays (JJAs). The thermal transport properties of crystalline and glassy solid states, above approximately 50 K, are considered alongside the electrical transport properties of JJAs across the superconductor-to-superinsulator transition.

Keywords: thermal conductivity, solidification, glass transition, quaternion order parameter, restricted dimensions, Kauzmann entropy paradox, BKT topological ordering

(Some figures may appear in colour only in the online journal)

1. Introduction

The origins of the anomalous temperature dependence of the thermal conductivity of non-crystalline materials, as compared with crystalline counterparts, have remained a matter of great interest over the past century [1–3]. In crystalline solid states, i.e. those that exhibit the translational periodicity of a lattice, heat conduction is due to the motion of collective elementary excitations known as phonons [4, 5]. Owing to the existence of a well-defined Brillouin zone, above approximately 50 K, phonons are scattered predominantly by resistive Umklapp phonon–phonon scattering processes. In this temperature range, the thermal conductivity increases with decreasing temperatures as resistive phonon–phonon interactions become less frequent. On the other hand, phonons cannot exist in non-crystalline solids that lack a well-defined Brillouin zone. The thermal conductivity of non-crystalline solids decreases with decreasing temperatures over the same temperature range [1, 6], and agrees well with Einstein's model of a random walk of thermal energy between neighboring groups of atoms [2, 7].

In this article, we approach the thermal conductivity as an emergent transport property that develops as a consequence of the mechanisms of solidification of undercooled atomic fluids. It is well-known that all solidifying atomic liquids in three-dimensions must undercool below the melting temperature T_M, in order to develop the necessary thermodynamic driving force (i.e. change in free energy) for the formation of a solid state. Within the context of thermodynamics, the degree of undercooling (prior to crystallization) is influenced by the rate of nucleation which depends on the size of atomic clusters and the surface energy associated with them. This work goes beyond thermodynamics, by approaching a topological framework for undercooling and solidification that is based on the notions of symmetry breaking. In particular, we focus on the influence of the topological structure of undercooled atomic fluids (that results due to atomic clustering) on the solidification process. In contrast to thermodynamics, for which the mechanisms of solidification are not directly connected to the transport properties of the solid state, it is by considering the role of topology that these phenomena may be related.

An original consideration of the topological nature of undercooling was offered by Frank [8], who suggested that undercooling below the melting temperature was related to an energetic-preference for icosahedral atomic clustering—which is incompatible with long-range crystallinity. More recent theoretical and topological approaches to undercooling [9–11], that build upon Frank's earlier work, have made use of the fact that particles with icosahedral coordination shells *do* tessellate the surface of a sphere in four-dimensions (despite the incompatibility of local icosahedral order with a space-filling arrangement). In approaching a more complete topological description of solidification in three-dimensions, this work builds upon these original concepts by adopting a quaternion orientational order parameter to characterize undercooled atomic liquids.

Our approach to solidification/melting in three-dimensions follows in the footsteps of original models of two-dimensional melting, proposed by Halperin and Nelson [12]. In these solidification/melting models, it is the topological ordering of an equilibrium concentration of topological defects (disclinations) that drives the formation of an orientationally-ordered crystalline solid state at low enough temperatures. Just as in the 2D case [12], we anticipate that three-dimensional crystalline solid states are achieved due to the formation of complementary disclination pairs which can be regarded as isolated dislocations [13–16]. Similar ideas [17], replacing disclinations with vortices (each are closed loop topological defects), have led to a theory of the phase transition towards low-temperature phase-coherent ground state of complex n-vector ordered systems (i.e. Bose–Einstein condensed superfluids) in two-dimensions. Ultimately, this topological framework points towards a novel interpretation of the inverse behavior of the thermal transport properties of crystalline and non-crystalline solid states above approximately 50 K.

Over the past decades, there has been a rapid development in understanding of the important role played by topology in the emergent transport properties of ordered systems [18–20]. For example, 2D and 1D complex ordered systems (i.e. superfluids) are prevented from developing conventional long-range order by spontaneous symmetry breaking (SSB) at finite temperatures [21] (Mermin–Wagner). Such systems, that are prevented from undergoing conventional ordering, must be considered to exist in 'restricted dimensions'. This is a consequence of the possible existence of a gas of misorientational fluctuations, that takes the form of spontaneously generated topological point defects. Still, in these scenarios of ordering in 'restricted dimensions,' a phase-coherent superfluid state may be achieved at finite temperatures as a result of a defect-driven topological ordering transition of the Berezinskii–Kosterlitz–Thouless (BKT) type [17, 22].

Herein, the notion of 'restricted dimensions' is extended to Bose–Einstein condensed ordered systems of particles whose internal degrees of freedom have the symmetry of quaternion numbers. This generalization is then applied to characterize orientational ordering in solidifying undercooled fluids, and derivative solid states in three-dimensions [11]. Just as conventional orientational order is prevented at finite temperatures for complex ordered systems that exist in $\mathbb{R}^2$, due to the existence of spontaneously generated topological point defects, so to is conventional orientational order prevented at finite temperatures for quaternion ordered systems that exist in $\mathbb{R}^4$ [23].

Going a step further, for n-vector ordered systems (e.g. complex 2-vector and quaternion 4-vector) that exist in 'restricted dimensions,' there is the possibility for the realization of distinct phase-incoherent ground states that are mirror images ('dual') to phase-coherent ground states [24]. Such scenarios of n-vector ordering in 'restricted dimensions' are well-modeled mathematically using $O(n)$ quantum rotor models, for which characteristics of the ground state are controlled by tuning a non-thermal parameter (g) that enters the Hamiltonian [25]. The most common examples of the manifestation of such phase-incoherent ground states are realized for thin-film charged Josephson junction arrays (JJAs), that are well-modeled using $O(2)$ quantum rotor models [24, 26–28]. In JJAs, the phase-incoherent ground state has

infinite electrical resistance [20] and acts as a mirror image of the phase-coherent superconductor (zero electrical resistance). In analogue, a non-thermal transition between orientationally-ordered (crystalline) and orientationally-disordered (non-crystalline) solid states is anticipated for a relevant $O(4)$ quantum rotor model. This leads to a topological interpretation of the thermal transport properties, of crystalline and non-crystalline solids.

The role played by topology in the solidification process is elucidated in section 2. In section 2.1, a quaternion order parameter space is introduced to characterize orientational order in undercooled atomic fluids. Section 2.2 reviews the topological principles that allow for the determination of available types of topological defects, and their dimensionality, in ordered systems. In section 2.3, the notion of 'Universality classes' that apply to Bose–Einstein condensates in 'restricted dimensions' are introduced within the context of $O(n)$ quantum rotor models. Using these topological principles, a viewpoint on crystallization is provided in sections 2.3.1 and 2.3.2—in the absence and in the presence of geometrical frustration. To complete the discussion of solidification processes, the glass transition is discussed in section 2.3.3. Finally, in section 3, the emergent thermal transport properties of solid states across the anticipated crystalline to non-crystalline transition are considered.

2. Topological origins of solidification

2.1. Quaternion orientational order parameter

At temperatures just below the melting temperature, orientational order in three-dimensional atomic fluids is characterized by the preferred orientational symmetry of atomic clustering [9, 11, 29, 30]. This is denoted by the subgroup of three-dimensional rotations $H \in G$, where $G = SO(3)$ is the full orientational symmetry group of the high-temperature liquid. In considering the topological properties of the ordered system, and in order to apply the theorems of homotopy [29, 30], it is important that the group G be simply connected (i.e. $\pi_1(G) = 0$). This larger group, that is simply connected, imbeds the continuous group G (that is not simply connected) and is called the 'universal covering group' of G. The most common example of such a relationship is between the three-dimensional group of proper rotations $SO(3)$ (not simply connected) and the special unitary group of degree two $SU(2)$ of unit quaternion elements [29, 30] (simply connected). The relationship between $SO(3)$ and $SU(2)$ is via a 2-to-1 homomorphism [29, 30], in which two quaternions correspond to each rotation in three-dimensions.

As a particular example of this 2-to-1 homomorphism, between $SO(3)$ and $SU(2)$, consider the case of preferred icosahedral coordination of atomic clustering about a central atom in three-dimensions $Y \in SO(3)$. As depicted in figure 1(A), atoms that express icosahedral coordination are unable to fill three-dimensional space; this phenomenon is known in the literature [31–33] as 'geometrical frustration'. However, particles with icosahedral coordination shells *do* tessellate the surface of a sphere in four-dimensions ($\mathbb{S}^3$) forming

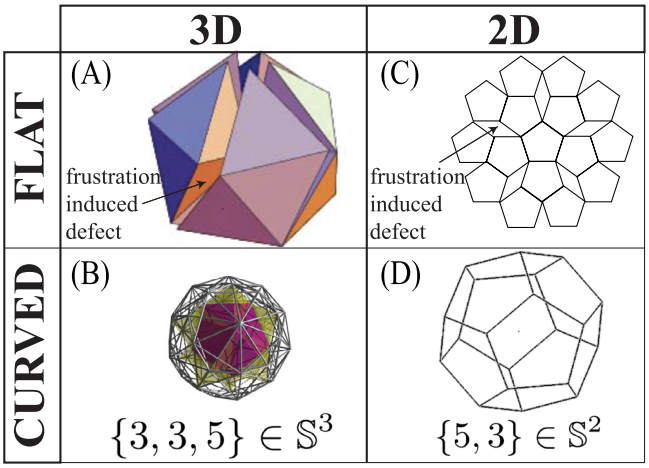

Figure 1. (A) and (C) are 'geometrically frustrated' tilings of 3D and 2D Euclidean (flat) space. Just as gaps remain between certain faces when regular tetrahedra are packed into 3D Euclidean space, there is no regular pentagonal tiling of the Euclidean plane. (B) and (D) are regular tessellations of the three-sphere ($\mathbb{S}^3 \in \mathbb{R}^4$) and the two-sphere ($\mathbb{S}^2 \in \mathbb{R}^3$), by the preferred short-range orientational order in (A) and (C).

a four-dimensional Platonic solid known as the $\{3,3,5\}$ polytope (figure 1(B)). The 120-vertices of the $\{3,3,5\}$ polytope are the elements of the binary representation [29, 30, 34] of $Y \in SO(3)$ in $SU(2)$. Similarly, although there is no pentagonal tiling of the plane (figure 1(C)) pentagons do tessellate the surface of a sphere in three-dimensions ($\mathbb{S}^2$) as a dodecahedron (figure 1(D)).

Ultimately, it is important to note that, as a consequence of the incompatibility of the preferred orientational order of atomic clustering with long-range order (due to short-range constraints [33] that impose geometrical frustration), there is a mismatch in the Gaussian curvature between flat space and the ideal curved space structure (figures 1(B) and (D)). It is this curvature mismatch that forces a finite density of topological defects into the flat space structure (figures 1(A) and (C)). These topological defects carry curvature that is proportional to the amount of curvature added to each cell in flat space in order to relieve the geometrical frustration [10].

In order to consider the topological properties of ordered systems, it is important to identify the relevant topological manifold $\mathcal{M}$ that characterizes the set of degenerate ground states that the ordered system can adopt:

$$\mathcal{M} = G/H. \tag{1}$$

In the particular case of solidification, below the melting temperature, atomic clustering breaks the group $G = SO(3)$ to a subgroup $H \in G$. The relevant simply connected group is $G = SU(2)$, such that:

$$\mathcal{M} = SU(2)/H' \tag{2}$$

where H' is the binary representation of H. Thus, the relevant orientational order parameter manifold in the solidification process ($\mathcal{M}$) can be identified with a subgroup of unit quaternion numbers, i.e. $SU(2)$, which gives an algebraic structure to the three-sphere $\mathbb{S}^3$. The group of unit quaternions, that give an algebra structure to the three-sphere (that resides in $\mathbb{R}^4$), is

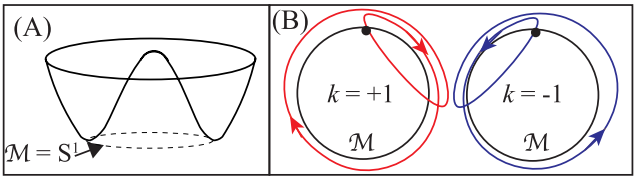

Figure 2. (A) The 'Mexican hat' potential energy configuration applies to complex ordered systems, below the bulk critical transition temperature. The manifold of degenerate ground states is the locus of points in the complex plane, i.e. $\mathcal{M} = \mathbb{S}^1$. (B) $\pi_1(\mathbb{S}^1)$ topological defects are available to complex ordered systems, by the specification of θ on some closed loop. If, on taking a closed loop in space, θ changes by $2\pi k$ ($k = 0, \pm1, \pm2, ...$ is the winding number) then a defect core exists within the circuit.

the next higher-dimensional algebra domain to the unit complex numbers—that give an algebra system to the unit circle in $\mathbb{R}^2$.

2.2. Topological defects, and their role in the theory of 'Universality classes' of phase transitions

2.2.1. Types of available topological defects. When studying phase transitions, e.g. solidification, it is often important to consider the role played by topological defects that are generated during the symmetry breaking process. Physical insight into the types of available topological defect elements can be gained by considering the topological properties of the relevant ground state manifold that applies to the ordered system (equation (1)). The ith homotopy group of $\mathcal{M}$, i.e. $\pi_i(\mathcal{M})$, describes the set of topological defect elements given by the possible mappings [14] of an i-dimensional sphere around $\mathcal{M}$. Non-trivial homotopy groups contain defect elements that, when drawn on $\mathcal{M}$, cannot be contracted to a point on its surface.

Returning to the general case of n-vector ordered systems that exhibit a continuous order parameter, the ground state manifold is $\mathcal{M} = S^m$ where $m = n - 1$. In these cases, the only non-trivial homotopy group of defects is [35]:

$$\pi_m(\mathcal{M}) = \mathbb{Z}, \tag{3}$$

where $\mathbb{Z} = 0, \pm1, \pm2, ...$ is a lattice of integers. Importantly, because of their identification with Z, the $\pi_m(\mathbb{S}^m)$ homotopy groups are necessarily Abelian [14]. Examples of Bose–Einstein condensed ordered systems that exhibit complex ($n = 2$) and quaternion ($n = 4$) n-vector order parameter are particularly interesting to consider. In complex 2-vector ordered superfluids, $\pi_1(\mathbb{S}^1)$ topological defects (known as vortices) are available [36] (figure 2). Similarly, $\pi_3(\mathbb{S}^3)$ topological defects are available to quaternion 4-vector ordered systems for which the order parameter resides in a four-dimensional vector space.

In real solidifying atomic systems, it is owing to the discrete nature of atomic clustering that the actual ground state manifold is not continuous (i.e. $\mathcal{M} = \mathbb{S}^3$) but instead has points identified on its surface: $\mathcal{M} = \mathbb{S}^3/H'$ where H' is the lift [29, 30] of $H \in G$ into $SU(2)$ (see equation (2)). This leads to the possible existence of topologically stable defect

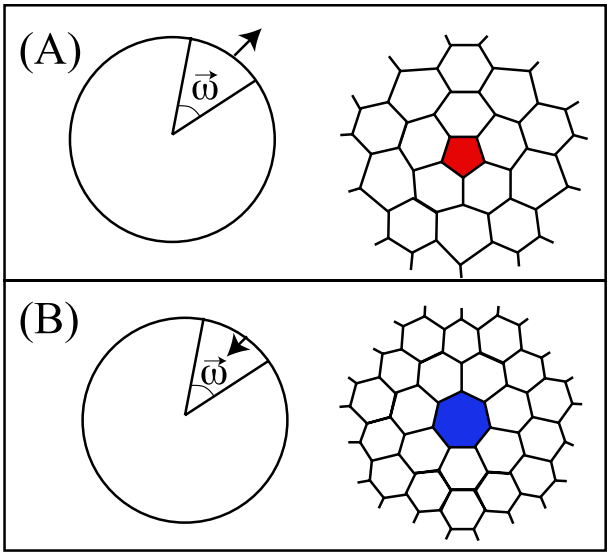

Figure 3. (A) Positive and (B) negative wedge disclinations in a honeycomb net. Wedge disclinations are characterized by a Frank vector ($\vec{\omega}$) topological invariant, on taking a measuring circuit around a point in space, and are the angular cousin to dislocations that are characterized by a linear Burger's vector. An angular deficit attributes a topological strength to a wedge disclination, by introducing positive or negative curvature to it that is concentrated at its core.

elements that belong to the fundamental homotopy group, i.e. that are identified by closed loops. These are wedge disclinations, that can be introduced by a standard Volterra process [37]. The Volterra process imparts an angular deficit (Frank vector) that can be measured as a topological invariant on taking a closed loop (measuring circuit) in the sample. This angular deficit concentrates curvature at the core of a wedge disclination defect. Figures 3(A) and (B) show examples of positive and negative disclinations in a 2D hexagonal net.

2.2.2. Dimensionality of available topological defects. Once the types of non-trivial homotopy groups of topological defects have been identified, it is important to consider how their dimensionality is influenced by the spatial dimension (D) in which the n-vector ordered system exists. This is because the dimensionality of the available topological defects plays an important role in the critical properties of ordered systems, in the vicinity of critical points. In general, defect elements that belong to the homotopy group $\pi_i(\mathcal{M})$, for ordered systems that exist in D spatial dimensions, have the dimensionality [35, 38, 39]:

$$d = D - i - 1. \tag{4}$$

Of note, for n-vector ordered systems, this expression tells us that $\pi_m(\mathbb{S}^m) = \mathbb{Z}$ topological defects ($m = n - 1$) are linear in $D = n + 1$ dimensions and are points in the dimension $D = n$. For ordered systems that exist in the dimension $D = n$, these point defects act to prevent conventional orientational order at finite temperatures. The particular case of $\pi_1(\mathbb{S}^1)$ vortices, available to complex 2-vector ordered systems (i.e. Bose–Einstein condensates), is shown in figure 4 (linear in 3D and,

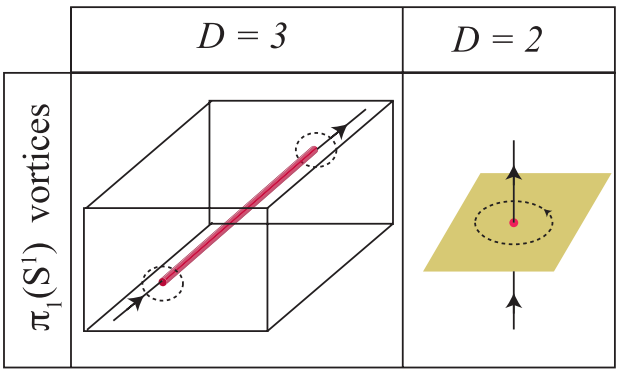

Figure 4. Vortices belong to the first homotopy group of $\mathcal{M} = S^1$, i.e. $\pi_1(\mathbb{S}^1) = \mathbb{Z}$. These topological defects are: linear defects in three-dimensions and, point defects in thin-films. (After [38]).

points in 2D). Similarly, $\pi_3(\mathbb{S}^3)$ topological defects, available to quaternion 4-vector ordered systems [23], are points in 4D and are linear in 5D.

In Bose–Einstein condensed n-vector ordered systems, as characterized by a complex or a quaternion orientational order parameter, the spatial dimension in which $\pi_m(\mathbb{S}^m) = \mathbb{Z}$ topological defects exist as points is referred to as the lower critical restricted dimension (D_{low}). This is the largest spatial dimension in which SSB is no longer possible at finite temperatures [19]. On the other hand, in ordered systems that exist in a bulk dimension larger than D_{low}, conventional orientational order can develop by SSB. This is a result of the higher-dimensional (linear) nature of $\pi_m(\mathbb{S}^m)$ topological defects available to n-vector ordered systems in bulk spatial dimensions (D_{bulk}). For Bose–Einstein condensed ordered systems that exist in D_{bulk}, the free energy cost to introduce linear $\pi_m(\mathbb{S}^m)$ topological defects is too high to permit them in the absence of applied external fields [18] such that their existence does not prevent SSB at finite temperatures.

Table 1 identifies the lower critical restricted dimension D_{low}, and bulk dimension D_{bulk}, for general Bose–Einstein condensates (characterized by broken complex ($\mathbb{C}$), quaternion ($\mathbb{H}$) or octonion ($\mathbb{O}$) symmetry). In these ordered systems of broken continuous symmetries, the *Nambu–Goldstone (NG) theorem* [40, 41] predicts the appearance of a set of massless NG-modes that correspond to the spontaneously broken internal symmetry generators. For example, a single NG-mode is anticipated in cases of broken $U(1)$ symmetry (complex) that is characterized by a single *generator*. Such complex 2-vector ordered systems are described mathematically using $O(2)$ models, and allow for the existence of vortex topological defects (i.e. $\pi_1(\mathbb{S}^1)$). Vortices are points in the *complex plane*, such that $D_{\text{low}} = 2$ for complex 2-vector ordered systems [19].

Similarly, three NG-modes are anticipated in cases of broken $SU(2)$ symmetry (quaternion) that is characterized using a set of three *generators*. In such quaternion ordered systems, third homotopy group topological defects ($\pi_3(\mathbb{S}^3)$) that are like higher-dimensional vortices are able to exist. These defect elements are points in the *quaternion plane*, such that $D_{\text{low}} = 4$ for quaternion 4-vector ordered systems. To summarize table 1, the lower critical restricted dimension for n-vector ordered systems that are characterized by one of the division algebras with continuous symmetries ($\mathbb{C}$, $\mathbb{H}$, $\mathbb{O}$) are 2D, 4D and 8D. A consequence of this is the realization of 2D, 4D and 8D quantum Hall effects [42, 43] whose fundamental structures are realized via these division algebras.

Table 1. Division algebras that exhibit continuous symmetries are: complex ($\mathbb{C}$), quaternion ($\mathbb{H}$) and octonion ($\mathbb{O}$) numbers. These numbers are n-vectors that have the dimensions: two- ($n = 2$), four- ($n = 4$) and eight- ($n = 8$). Ordered systems characterized by these n-vectors may be described using $O(n)$ models in D-dimensions. The relevant manifold of degenerate ground states is: $\mathcal{M} = S^m \in \mathbb{R}^n$ where $m = n - 1$, since the amplitude of the order parameter is roughly constant at any given temperature. On spontaneous symmetry breakdown of a continuous symmetry, the Nambu–Goldstone (NG) theorem anticipates the appearance of m massless NG-modes [40, 41]. $\pi_m(\mathcal{M})$ topological defects are available to such ordered states. In the lower critical dimension D_{low}, these defects exist as spontaneously generated point defects that prevent the development of conventional orientational order by SSB.

Algebra domain:	Model:	$S^m \in \mathbb{R}^n$	NG-modes:	Defect:	D_{low}	D_{bulk}
$\mathbb{C}$ (U(1))	O(2)	$S^1 \in \mathbb{R}^2$	1	$\pi_1(S^1)$	2	3
$\mathbb{H}$ (SU(2))	O(4)	$S^3 \in \mathbb{R}^4$	3	$\pi_3(S^3)$	4	5
$\mathbb{O}$ (SU(3))	O(8)	$S^7 \in \mathbb{R}^8$	7	$\pi_7(S^7)$	8	9

Similar considerations of ordering in bulk and 'restricted dimensions' were presented for the simplest example of symmetry breaking in the discrete $\mathbb{Z}_2$ Ising model, characterized by the real number ($\mathbb{R}$) domain, in the first half of the 20th century. In the Ising model, the global symmetry is the $\mathbb{Z}_2$ transformation [19] that exchanges 'up' and 'down'. As a consequence of this discrete symmetry of the $\mathbb{Z}_2$ Ising model, there is an absence of Nambu–Goldstone modes [41]. Therefore, the only topological defects that are available belong to the $\pi_0(\mathbb{Z}_2)$ homotopy group. These topological defects act to prevent global orientational order at finite temperatures in the 1D Ising model, which has no conventional phase transition (1925, [44]). These topological arguments point towards a conventional phase transition in 2D 'bulk' $\mathbb{Z}_2$ Ising models, for which $\pi_0(\mathbb{Z}_2)$ topological defects are linear (see equation (4))—this agrees with the modeling of Onsager (1944, [45]).

2.3. (D, n) 'Universality classes' and O(n) quantum rotor models in 'restricted dimensions'

As discussed in detail in section 2.2.2, the spatial dimension of an n-vector ordered system (D) greatly influences its long-range order (LRO) properties and this has its origins in the topology of the ground state manifold $\mathcal{M}$. In general, Bose–Einstein condensed (n-vector) ordered systems that exist in the lower critical restricted dimension belong to the (D, n) 'Universality class'[1] where $D = D_{\text{low}} = n$. These ordered systems are

[1] The 'Universality hypothesis' predicts that the critical behavior of all n-vector ordered systems that exist in D dimensions, i.e. that belong to the same (D, n) 'Universality class,' will be the same in the vicinity of critical points [19].

well-described using n-dimensional $O(n)$ quantum rotor models [25]. The question of understanding the possible low-temperature ordered states that are able to exist in 'restricted dimensions' remains an important problem in condensed matter physics [19], and is explored in this section.

Critically, $O(n)$ quantum rotor model Hamiltonians consist of both potential and kinetic energy terms that cannot be minimized simultaneously. While the potential energy term favors a ground state of perfectly aligned order parameters, and establishes phase-coherency (i.e. orientational ordering) at low-temperatures, the kinetic energy term favors the localization of condensed particles and a maximally orientational-disordered low-temperature state (driven by the Heisenberg uncertainty principle [25]). It is the competition between these two energy terms that leads to a diverse spectrum of ground states for Bose–Einstein condensed n-vector ordered systems that exist in 'restricted dimensions'. A topological viewpoint on the formation of perfectly orientationally-ordered ground states, in the absence of kinetic energy effects (i.e. the classical limit), is described in section 2.3.1. Geometrically-frustrated crystalline solid states, that form in the limit of finite kinetic energy effects, are introduced in section 2.3.2. Lastly, in section 2.3.3, glass formation is discussed as a dual transition to crystallization.

2.3.1. Classical defect-driven topological BKT transitions. In the range of dominant potential energy, of the relevant $O(n)$ quantum rotor model, a plasma of spontaneously generated mobile topological defects develops just below the bulk critical transition temperature that prevents the formation of a phase-coherent ground state [27, 46]. Despite the prevention of long-range order at finite temperatures (Mermin–Wagner theorem), an orientationally-ordered low-temperature state can develop (above 0 K) by the minimization of potential energy via a defect-driven BKT topological ordering transition [17, 22, 23]. A topological transition may be anticipated in these scenarios because the available $\pi_m(\mathbb{S}^m) = \mathbb{Z}$ topological defects are necessarily Abelian [14], such that the rule for their combination is the addition of their topological strengths (e.g. winding number). Bound pairs of topological defects, whose strengths sum to zero, are known as 'sum-0' pairs and are topologically equivalent to the uniform state. Classical defect-driven BKT transitions, via the binding of $\pi_m(S^m)$ topological defects (in $O(2)$ and $O(4)$ quantum rotor models) and of wedge disclinations in solidifying systems are discussed in sections 2.3.1.1 and 2.3.1.2.

2.3.1.1.Binding of $\pi_m(S^m)$ topological defects. Evidence for a higher-dimensional defect-driven BKT transition in four-dimensional $O(4)$ quantum rotor models, in analogue to the prototypical defect-driven BKT transition in 2D $O(2)$ quantum rotor models, has recently been provided by the authors [23]. These defect-driven BKT transitions in the classical limit, in 2D $O(2)$ rotor models and 4D $O(4)$ rotor models, are discussed below. In considering real solidifying atomic system, that exhibit atomic clustering, it is furthermore important to extend beyond this recent work by discussing the binding of complementary wedge disclination elements on the formation of atomic lattices (section 2.3.1.2).

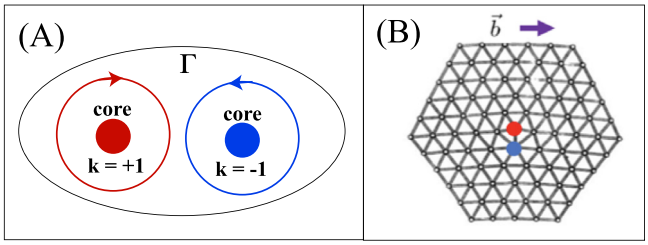

Figure 5. (A) A loop Γ that surrounds a pair of point defect cores whose topological invariants sum to zero is topologically equivalent to the uniform state, because $\pi_m(S^m)$ defects are Abelian. (B) A dipole of positive and negative wedge disclinations, and the Burger's circuit and Burger's vector used to define the equivalent edge dislocation. (B) reprinted figure with permission from [15], copyright 2018 by the American Physical Society.

Complex $O(2) \sim S^1$ ordered systems. A most notable example of a defect-driven BKT-transition towards a phase-coherent ground state occurs for 2D $O(2)$ JJAs. A cartoon depicting the formation of a 'sum-0' pair of point defects in such complex ordered systems in two-dimensions (i.e. $\pi_1(\mathbb{S}^1) = \mathbb{Z}$) is shown in figure 5(A). In order to determine the critical transition temperature, at which these 'sum-0' bound pairs become energetically favorable, one must consider the minimization of the potential energy that arises due to coupling between nearest-neighbor $O(2)$ rotors that represent complex order parameters. The orientation of each $O(2)$ rotor, located at site i, is determined by its scalar phase angle parameter $\theta_i \in [0, 2\pi]$. Thus, the potential energy term of $O(2)$ rotor models has the form:

$$\hat{V} = -J \sum_{\langle ij \rangle} \cos(\theta_i - \theta_j), \tag{5}$$

where J is the interaction energy between nearest-neighbors that interact across weak-links, and the sum is taken over all nearest-neighbor interactions $\langle ij \rangle$. Misorientational fluctuations in these scalar phase angles (θ_i) throughout the system take the form of a gas of topologically stable point defects ($\pi_1(S^1)$ vortices) that must undergo a topological ordering event in order to allow for the existence of a phase-coherent state at finite temperatures [17, 47].

Quaternion $O(4) \sim S^3$ ordered systems. Quaternion ordered systems in four-dimensions are higher-dimensional analogues of 2D $O(2)$ JJAs. In the range of dominant potential energy, in analogue to 2D $O(2)$ JJAs, a defect-driven BKT transition of third homotopy group topological point defects is anticipated to allow for the existence of an orientationally-ordered low-temperature state [23]. Below the bulk critical transition temperature, the orientation of each $O(4)$ rotor is determined by the state of three scalar phase angle parameters ($\theta \in [0, \pi], \theta_1 \in [0, \pi], \theta_2 \in [0, 2\pi]$) such that the potential energy term has the form [23]:

$$\hat{V} = -J \sum_{\langle ij \rangle} (\cos\theta_i \cos\theta_j + \sin\theta_i \sin\theta_j \times (\cos\theta_{1,i} \cos\theta_{1,j} + \sin\theta_{1,i} \sin\theta_{1,j} [\cos(\cos\theta_{2,i} - \cos\theta_{2,j})])). \tag{6}$$

This expression is a direct higher-dimensional analogue to equation (5). As the temperature of this ordered system is

lowered towards 0 K, equation (6) is minimized by a ground state of perfectly aligned $O(4)$ rotors that represent the field of order parameters throughout the 4D array. This ground state of perfectly aligned rotors is achievable by a binding event within the gas of $\pi_3(S^3)$ topological defects [23].

2.3.1.2.Binding of $\pi_1(\mathcal{M})$ wedge disclinations. In real solidifying atomic systems, owing to the discrete symmetry of atomic clustering, wedge disclination topological defects (fundamental homotopy group, figure 3) are also present in the gas of misorientational fluctuations that develops below the melting temperature. Because disclination topological defects belong to the fundamental homotopy group, following equation (4), they are: point-like in 2D, linear in 3D and planar in 4D. In 3D, disclination lines are created by connecting measuring circles surrounding points in a plane [49] along a line.

Just like third homotopy group defects, wedge disclinations are topologically stable when drawn on $\mathcal{M} = \mathbb{S}^3/H'$ and therefore must undergo a topological ordering process in order to allow for the realization of an orientationally-ordered crystalline solid state at low temperatures. Pairs of low-energy complementary wedge disclinations (figure 5(B)), that are favored energetically (over isolated wedge disclinations) below the finite temperature that marks crystallization, are considered to be edge dislocations [13–16] that belong to the fundamental homotopy group of the order parameter space of the crystalline solid state.

During the crystallization process, it is important to consider how the topological properties of the ordered system changes. Topology is concerned with the properties of a manifold ($\mathcal{M}$) that are preserved under continuous deformations. A particularly important topological invariant property is the genus (h) of $\mathcal{M}$, that measures the number of ways that you can cut slices of $\mathcal{M}$ without it falling apart (often described as the number of holes in $\mathcal{M}$). Topologically, all manifolds $\mathcal{M}$ are classified according to their genus which has a strong relationship to the curvature of the surface. In particular, on crystallization, the order parameter space changes from S^3/H' in the undercooled liquid to T^3 in the crystalline solid state. This change in topology points towards the binding of wedge disclinations (that carry curvature) into edge dislocations (that carry no curvature).

The total curvature of a surface can change only if its topology changes, for instance, by adding a handle to the surface in order to change its genus (figure 6(A)). The relationship between topology and curvature is most easily seen by considering two-dimensional orientable surfaces (e.g. $\mathbb{S}^2$ and $\mathbb{T}^2$), for which the relationship between the genus and curvature of a surface ($\mathcal{M}$) follows the Gauss–Bonnet theorem:

$$\int_{\mathcal{M}} K \mathrm{d}A = 2\pi\chi \tag{7}$$

where $\chi = 2(1-h)$ is the Euler characteristic of $\mathcal{M}$, and K is its Gaussian curvature.

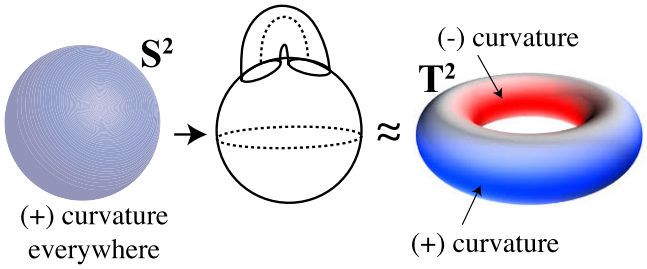

Figure 6. An m-dimensional sphere ($\mathbb{S}^m$) can be transformed into an m-dimensional torus ($\mathbb{T}^m$) by 'adding a handle' to the surface, i.e. the genus of $\mathbb{T}^m$ is one while the genus of $\mathbb{S}^m$ is zero. This is shown here in two-dimensions. The surface without handles ($\mathbb{S}^m$) has positive integral Gaussian curvature, while the total curvature of the surface with a single handle ($\mathbb{T}^m$) is zero no matter how the surface is deformed.

Consider the two-dimensional sphere ($\mathbb{S}^2$), for example, for which the Gaussian curvature is constant everywhere. By equation (7), the integral of the Gaussian curvature is just the area times the constant positive curvature (i.e. $4\pi R^2 \cdot 1/R^2 = 4\pi$) such that the Euler characteristic of a two-dimensional sphere is $\chi = 2$. By adding a single handle to an n-dimensional sphere, one obtains an n-dimensional torus (see figure 6(A)) whose Euler characteristic is zero (i.e. $\chi = 0$). By equation (7), such a surface (that has the topology of a sphere with a single handle) has zero integral curvature [50]. This is true no matter how the surface is deformed, such e.g. an n-dimensional torus and an n-dimensional coffee mug (with a single handle) are homeomorphic.

On crystallization, a ground state of ideal lattice points develops that is characterized by a well-defined Brillouin zone (primitive cell in reciprocal space) in D-dimensions. The Brillouin zone exhibits periodic boundary conditions (Born–von Karman [4]), and acts to define the momentum order parameter space of the crystalline lattice. For crystalline solid states, owing to these periodic boundary conditions (Born–von Karman), the topology of the order parameter space is a D-dimensional torus. A two-dimensional example is shown in figure 7(A), for which a two-dimensional torus is obtained by gluing opposite edges of a 2D Brillouin zone together according to boundary conditions.

The change in topology of the order parameter space during the crystallization process (i.e. the development of a ground state of translational order from an undercooled atomic liquid) may be viewed as akin to the adding of a handle onto the orientational order parameter space of the undercooled atomic liquid. The change in topology of the order parameter space at the crystallization transition in three-dimensions follows directly from the two-dimensional example depicted in figure 6(A). The order parameter space of a three-dimensional crystalline solid state is a three-dimensional Brillouin zone with periodic boundary conditions (figure 7(B)). A three-dimensional torus ($\mathbb{T}^3$) is obtained when the opposite faces are glued together according to the boundary conditions.

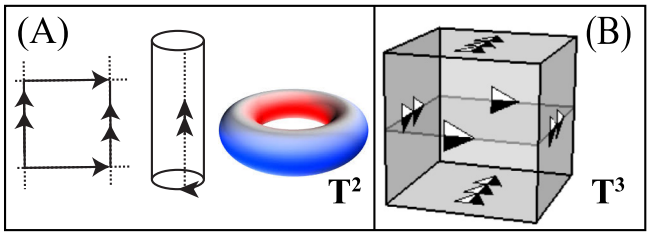

Figure 7. (A) A generic 2D Brillouin zone, with maximum wavevectors k_x and k_y. Owing to periodic boundary conditions that apply to the first Brillouin zone, it has the topology of a two-dimensional torus $\mathbb{T}^2$. (B) A generic 3D Brillouin zone, with periodic boundary conditions.

Owing to the development of translational periodicity (i.e. a well-defined Brillouin zone), the thermal entropy due to the displacement of atoms away from their ideal lattice positions at finite temperatures is characterized by the density of collective excitations (known as phonons). In real three-dimension crystalline solids, phonons are the three anticipated Nambu–Goldstone modes of broken quaternion symmetry that are classified as 1 longitudinal mode (compression waves) and 2 transverse modes (shear waves) per condensed atom. The spectrum of phonons describe the energy cost to perform certain allowable atomic displacements from the crystalline ground state, owing to the rigidity of the ordered system. Atomic displacements that give rise to phonon collective excitations can be drawn on the surface of $\mathcal{M}$, and may always be contracted to a point on its surface; in this way, phonon excitations are unique from topological defects, which are topologically stable on the surface $\mathcal{M}$.

In addition to elementary excitations in crystalline solid states (phonons), *topological defects* in the translational order parameter field (i.e. dislocations) may also be present at finite temperatures. As noted earlier, the order parameter space of a crystalline solid, is an n-dimensional torus shape ($\mathbb{T}^n$). Topologically, n-dimensional tori are homeomorphic to the Cartesian product of n circles: $\underbrace{\mathbb{S}^1 \times ... \times \mathbb{S}^1}_{n}$. It follows that, the fundamental homotopy group of $\mathbb{T}^n$ is isomorphic to the product of the fundamental homotopy group of n circles [50]. Hence, the fundamental homotopy group in three-dimensional crystalline solids is:

$$\pi_1(\mathbb{T}^3) = \mathbb{Z} \times \mathbb{Z} \times \mathbb{Z}, \tag{8}$$

where $\mathbb{Z}$ represents the set of all arbitrary integers. That is, a dislocation defect in three-dimensions is labeled by a set of three integers (b_u, b_v, b_w) that identify the magnitude of the Burger's vector in the x-, y- and z-directions.

Two dimensional examples of dislocations are shown in figure 8, for which the field of atomic displacements that is introduced in the vicinity of a dislocation defect core corresponds to a loop around the hole of a two-dimensional torus. Rearranging the atoms slightly deforms the loop but does not change the number of times it wraps around the hole; this is why a dislocation is a topological defect. Importantly, unlike π_1 disclinations, π_1 dislocations carry no curvature.

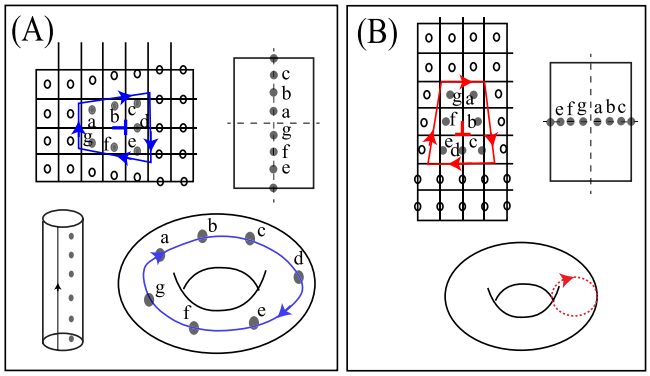

Figure 8. Dislocation fundamental homotopy group defects are permitted in crystalline solids. As a closed loop is traversed around a dislocation, the positions of atoms drift with respect to their ideal lattice positions. This corresponds to a loop around the order parameter space. Rearranging the atoms slightly deforms the loop, but does not change the number of times it wraps around the torus. (A) A loop around a dislocation that corresponds to an extra row of atoms corresponds to a path that passes around the hole of the torus. (B) A path through the hole of the torus corresponds to an extra column of atoms. Reproduced with permission of the Licensor through PLSclear, from [36]. Copyright Oxford University Press 2006.

Topologically, this is a fundamental consequence of the fact that a torus, i.e. a sphere with a single handle, upon which dislocation closed-loop defects are defined have zero integral Gaussian curvature. Because the n-dimensional torus has zero integral Gaussian curvature, any closed-loop topological defect that is defined upon its surface is also flat, i.e. it carries no curvature.

Thus, it is anticipated that, pairs of complementary wedge disclination defects (with equal and opposite angular deficit) bind together at the finite temperature that marks crystallization. These bound pairs of complementary wedge disclinations, that are topologically stable as isolated defects in the undercooled atomic liquid, are topologically equivalent to edge dislocations that are characterized by a Burger's circuit (figure 5(B)). Isolated wedge disclinations are only able to persist within the solid state in the event of geometrical frustration [11, 32] (figure 1), as will be discussed more completely in section 2.3.2.

2.3.2. Geometrical frustration: the major skeleton network in topologically close-packed crystalline solids. The role of geometrical frustration is to introduce finite kinetic energy effects into the relevant $O(4)$ quantum rotor model Hamiltonian. Thus, in the range of dominant potential energy, geometrical frustration may be viewed as akin to magnetic frustration that can be realized in charged $O(2)$ Josephson junction arrays in the presence of an applied magnetic field [52]. In $O(2)$ Josephson junction arrays, in the absence of an applied magnetic field, the concentrations of topological defects with equal and opposite signs are equal [27, 52]. The entire concentration of topological defects binds into low-energy paired configurations below a critical temperature, via a BKT transition, and no unpaired topological defects persist to the ground state. Similarly, in the absence of geometrical

frustration, crystalline ground states are achieved by a defect-driven BKT-like transition and are not plagued by topological defects.

Geometrical frustration is evident in three-dimensions when the preferred orientational order of atomic clustering ($H \in SO(3)$) is incompatible with a space-filling crystal [11, 32] (e.g. figure 1(A)). Geometrical frustration, evident in flat space, is relieved by allowing for positive curvature to enter into each of the atomic clusters [53]. This produces a tessellation of the three-dimensional space of constant positive curvature, as $\mathcal{M} = \mathbb{S}^3/H'$, that is known as a polytope [11] (e.g. figure 1(B)). In cases of geometrical frustration, owing to a curvature mismatch between the tessellation of $\mathcal{M}$ and flat space, $\mathcal{M}$ cannot be flattened into Euclidean space without the introduction of topological defects.

With the incorporation of geometrical frustration, the finite positive Gaussian curvature that is attributed to each geometrically frustrated atomic vertex drives an asymmetry in the plasma of disclination defects towards those that concentrate negative curvature at their core [32, 54, 55]. These excess negative disclinations balance out the positive curvature that is attributed to geometrically frustrated atomic vertices. Thus, in cases of geometrical frustration, the biased nature of the plasma of disclinations ensures that the three-dimensional Euclidean space remains flat on average [9, 11].

The incorporation of finite kinetic energy effects, in the presence of geometrical frustration, also biases the plasma of third homotopy group defects. This is akin to the shifting of the vortex–antivortex plasma in charged $O(2)$ Josephson junction arrays that express magnetic frustration in the presence of an applied magnetic field [27, 52]. In the range of dominant potential energy, in solidifying undercooled atomic liquids that are geometrically frustrated, excess negatively signed topological defects are unable to form low-energy paired configurations on crystallization and will persist to the solid ground state. In the solid state, these unpaired topological defects are pinned within a periodic arrangement so that the crystalline ground state is one of zero configurational entropy.

In three-dimensional geometrically frustrated crystalline solids, the periodic arrangement of negative disclination lines is known as the ordered major skeleton network [9, 56, 57]. In general, geometrically frustrated crystalline structures are known as topologically close-packed (TCP) crystals which, in contrast to FCC and HCP packings, are comprised exclusively of tetrahedral interstices [58], i.e. without octahedral interstices. Frank–Kasper structures [56, 57] are a particular example of TCP crystalline solid states in three-dimensions, that express preferred icosahedral local orientational order ($Y \in SO(3)$). Figure 9(A) depicts an example of the ordered major skeleton network in a 3D Frank–Kasper structure. In the presence of geometrical frustration, because topological defects persist to the crystalline ground state it is no longer one of perfect orientational order. That is, the set of scalar phase angle parameters that characterize the orientational order parameter will vary from site

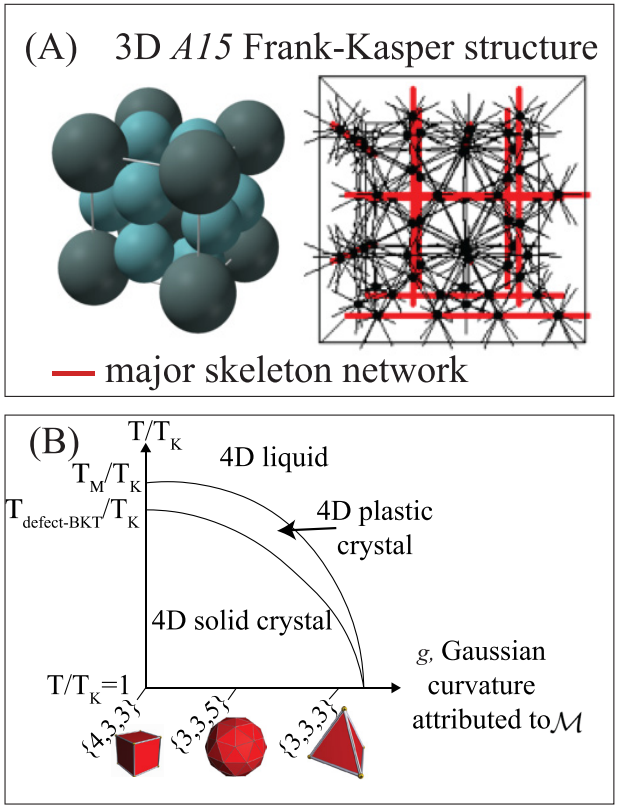

Figure 9. (A) *A*15 structures are one of the most common of the Frank–Kasper family of TCP phases. Three orthogonal grids of $Z = 14$ coordinated atoms, which are $-72°$ disclination lines [9], comprise the ordered major skeleton network in *A*15 compounds. Reproduced from [51]. © IOP Publishing Ltd. All rights reserved. (B) Anticipated solidification phase diagram of a 4D plastic crystal, in coordinates T versus geometrical frustration, in the range of dominant potential energy. A defect-driven BKT transition, at $T_{\text{defect-BKT}}$, separates the plastic crystal phase (i.e. undercooled liquid below T_{M}) from the crystalline solid state. Solidification occurs at a finite temperature, even in the limit of critical geometrical frustration for which a solid state forms at the Kauzmann temperature (T_{K}).

to site in order to facilitate the incorporation of frustration-induced topological defects.

Figure 9(B) depicts an anticipated phase diagram that applies to 4D $O(4)$ quantum rotor models, in the range of dominant potential energy, in coordinates of reduced temperature versus geometrical frustration. Notably, the quantity of geometrical frustration is not a continuous variable because the preferred orientational symmetry of atomic clustering $H \in SO(3)$ is a discrete subgroup of $G = SO(3)$. For geometrically frustrated atomic clusters, the positive Gaussian curvature attributed to each atomic vertex is inversely proportional to the radius [10] of $\mathcal{M} = \mathbb{S}^3/H'$. That is, if fewer vertices are identified (i.e. for smaller discrete symmetry groups $H \in SO(3)$) the radius of $\mathcal{M}$ is smaller and consequently the positive Gaussian curvature that is attributed to each geometrically frustrated atomic vertex increases.

With increasing geometrical frustration, the plasma of topological defects becomes increasingly biased and the

crystallization transition temperature is suppressed. Increasing geometrical frustration towards a critical value causes the spacing between topological defects to become reduced until the ground state is no longer crystalline. The suppression of crystallinity, at a critical value of geometrical frustration, is a higher-dimensional analogue to the suppression of the superconducting ground state of charged $O(2)$ JJAs at the superconductor-to-superinsulator transition [24, 46].

2.3.3. Dual BKT transition (glass transition). Herein, it is suggested that glass formation is driven by the minimization of the kinetic energy term of $O(4)$ quantum rotor models that describe orientational ordering in solidifying systems. These orientationally-disordered low-temperature solid states are anticipated to be 'dual' to crystalline solid states (as a consequence of Heisenberg uncertainty relations [25] that apply to the model).

Just below the melting temperature, internal relaxations by molecular rearrangements within a glass-forming liquid are necessary to remain in the undercooled state (metastable equilibrium). These internal relaxations are thermally activated, such that average structural relaxation times follow Arrhenius's law [59]. As the temperature is lowered below some critical value, the glass transition temperature, the undercooled system will fall out of metastable equilibrium and form an orientationally-disordered solid state[2] that can resist shear deformations.

A maximally orientationally-disordered low-temperature solid state is obtained in the absence of potential energy effects. Maximal orientational disorder implies that all condensed particles should become thermally pinned at the glass transition. This solidification process may be considered as akin to the formation of neutral charge dipoles at the dual-BKT transition towards the phase-incoherent superinsulating low-temperature state in charged $O(2)$ JJAs [60]. In this way, non-crystalline solid states should be viewed as higher-dimensional (uncharged) analogues to superinsulating ordered states of Cooper pairing [24, 28] that can be realized in O(2) JJAs. With the incorporation of finite potential energy effects, the glass transition temperature becomes suppressed so that the system may become increasingly undercooled. This is possible because coupling between neighboring atomic clusters (potential energy effects) enables internal relaxations that are necessary to ensure an adequate sampling of configurations, such that the undercooled system remains ergodic [61] to lower temperatures.

In the laboratory, the cooling rate is the most obvious tuning parameter that can be utilized to drive a glass-forming system to become increasingly undercooled (see figure 10(A)). In the hypothetical limit of an infinitely slow cooling rate, an undercooled system may become entirely internally relaxed and form an 'ideal glass' at the well-known [62–66] Kauzmann point (T_K). This hypothetical 'ideal glass' exhibits the maximum orientational correlations of any solid glass structure, yet is not translationally ordered. At the Kauzmann point,

[2] By convention, glass formation occurs as the viscosity rises above a critical value (10^{13} Poise).

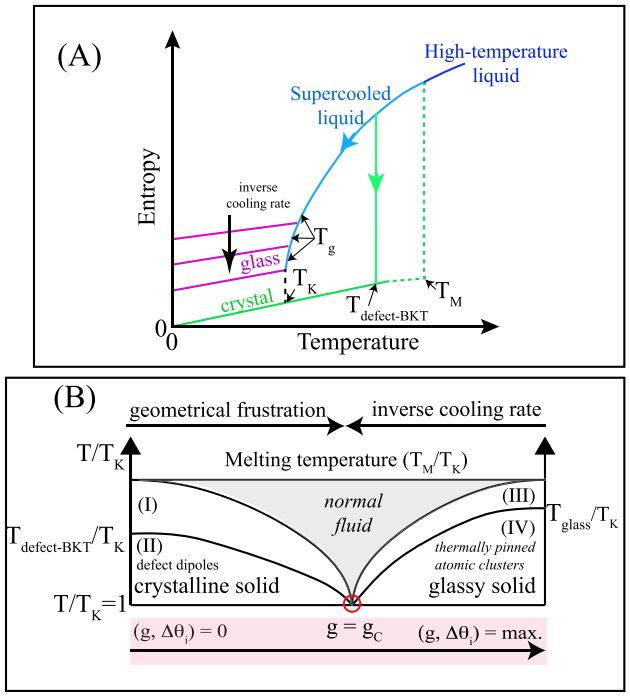

Figure 10. (A) With slower cooling rates, glass-formers can become increasingly undercooled. An entropy paradox occurs in the limit of an infinitesimal cooling rate, at the Kauzmann temperature (T_K) that represents an 'ideal glass transition'. Any real glass transition occurs at a higher temperature (T_g), as a supercooled liquid freezes. (B) Schematic phase diagram for solidification of undercooled atomic liquids, using an $O(4)$ quantum rotor model, plotted in coordinates of T (normalized by T_K) versus the ratio of importance of kinetic and potential energies (g). A 'self-dual' critical point (open circle) is identified at the Kauzmann point (i.e. at $g = g_C$ and $T = T_K$).

a paradox arises wherein the difference in configurational entropy of the 'ideal' non-crystalline system and its crystalline counterpart is zero. However, in physical systems, this 'ideal glass transition' is never reached because it would require a cooling rate longer than the duration of the Universe [61, 67] to achieve and so any real glass transition occurs at a higher temperature.

At the glass transition, condensed atomic particles that are not internally relaxed become thermally pinned. Thus, by the inclusion of finite potential energy effects, there is a trade-off between the thermal pinning of condensed particles at the glass transition (that are not internally relaxed) and the development of orientational correlations between neighboring atomic clusters (by internal relaxations prior to glass formation). This can be viewed as a consequence of the symmetric uncertainty relations [25], between the amplitude and scalar phase angle parameters, that apply to the $O(4)$ quantum rotor model. These arguments follow as an extension of the quantum-mechanical arguments for the possibility of the existence of a superinsulating low-temperature state of charged $O(2)$ JJAs [24, 28]. In terms of our topological viewpoint on solidification, the 'ideal glass transition' (at the Kauzmann point) may be viewed as a solidification process that occurs at the 'self-dual' critical point belonging to the $O(4)$ quantum rotor model (at which the potential and kinetic energy terms become comparable).

2.3.4. Anticipated phase diagram for 3D solidification. Figure 10(B) depicts the anticipated phase diagram for three-dimensional solidification, across a crystalline-to-noncrystalline transition, plotted in coordinates temperature (normalized by the finite Kauzmann temperature, T_K) versus the ratio of importance of kinetic and potential energies g (dimensionless). In three-dimensions, the crystallization and glass transition temperatures converge at a finite temperature (T_K) at the 'self-dual' critical point. This corresponds to a first-order transition between crystalline and glassy solid states [28].

On the phase diagram (figure 10(B)), in the range of dominant potential energy a defect-driven BKT transition separates an undercooled system (Region (I)) from a low-temperature orientationally-ordered (crystalline) solid state (Region (II)). In the absence of kinetic energy effects, a crystalline ground state is favored that is free of topological defects ($\Delta\theta_i = 0$ for $i = 0, 1, 2$). In the range of dominant potential energy, geometrical frustration skews the concentration of topological defects towards those of a particular sign and the ground state becomes topologically close-packed (e.g. Frank–Kasper structures). In these geometrically frustrated crystalline solid states, the uncertainty in the scalar phase angles throughout the system is no longer zero. Geometrical frustration suppresses the defect-driven crystallization transition temperature towards a minimum in the limit of critical geometrical frustration.

In the range of dominant kinetic energy, just below the melting temperature, an undercooled liquid forms in which there is little interaction between atomic clusters (Region (III)). The glass transition temperature, which marks the freezing of this undercooled system into a particular non-equilibrium configuration (Region (IV)), is sensitive to the cooling rate. In the absence of interactions between atomic clusters, in cases of arbitrarily fast cooling rates, a maximally orientationally-disordered solid state ($\Delta\theta_i = \max.$ for $i = 0, 1, 2$) is obtained. In contrast, non-crystalline solid states that form in the hypothetical limit of an infinitely slow cooling rate (i.e. an 'ideal glass') are realized at the 'self-dual' critical point (i.e. Kauzmann point) and are therefore entirely internally relaxed, yet lack translational order.

3. Emergent thermal transport properties

The thermal properties of solid state systems are intimately related to the structure that forms from the undercooled atomic liquid. In particular, from a topological viewpoint, the inverse temperature dependence of the thermal conductivity of crystalline and non-crystalline solid states (above approximately 50 K) may be viewed as a consequence of the realization of 'dual' low-temperature states of $O(4)$ quantum rotor model Hamiltonians. It follows that the thermal transport properties of solid states are analogous to the well-studied electrical transport properties of charged $O(2)$ JJAs [20], which display a singularity at the superconductor-to-superinsulator transition [24] (figure 11(A)). Likewise, a singularity in the thermal transport properties as a function of temperature is anticipated at the 'self-dual' critical point in $O(4)$ quantum rotor models.

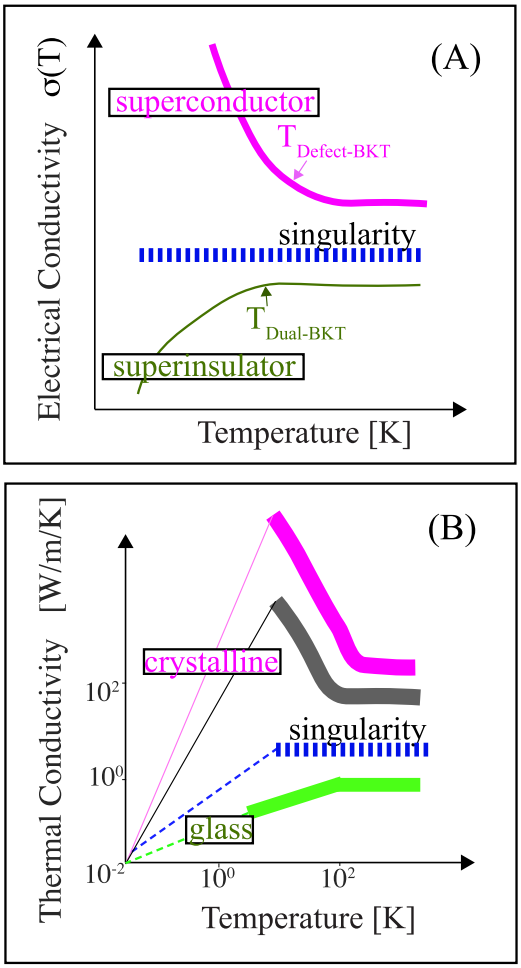

Figure 11. (A) The superconductor-to-superinsulator transition in $O(2)$ Josephson junction arrays is displayed in the temperature dependence of the electrical conductivity. A superconductor forms in the range of dominant potential energy, and a superinsulator, which exhibits 'zero electrical resistance' is preferred in the range of dominant kinetic energy. (B) Anticipated thermal conductivity (κ), across a transition between crystalline and non-crystalline ground states, above approximately 50 K. With the incorporation of geometrical frustration into the crystalline ground state, the overall magnitude of κ should become suppressed. In contrast to crystalline solids, κ of non-crystalline solids decreases with decreasing temperatures. The magnitude of κ of non-crystalline solids is anticipated to be proportional to the degree of internal relaxation prior to glass formation.

Anticipated thermal conductivities of crystalline and non-crystalline solid states, above approximately 50 K, are shown in figure 11(B). In the absence of geometrical frustration, a perfect crystalline ground state that is free of topological defects is achieved for which the thermal conductivity rises to a maximum value (pink) before falling to zero at 0 K. In the presence of geometrical frustration, frustration induced topological defects that are periodically arranged in the ground state generate a finite uncertainty in the global orientational order parameter field. This leads to the suppression of the overall thermal conductivity (grey).

With a critical value of geometrical frustration, the ground state is no longer crystalline and characteristic features of

translational order are no longer displayed in the thermal transport properties. This leads an anticipated a singularity in the thermal transport properties at the 'self-dual' critical point (dashed). Despite lacking translational order, this system does express orientational order and therefore acts as a bridge between the crystalline and non-crystalline structures. This hypothetical non-crystalline solid state (i.e. 'ideal glass'), should present thermal transport properties that are similar to quasicrystals (which have orientational order but not translational order). The thermal transport properties of quasicrystalline materials have been shown to be comparable to those observed in amorphous systems [68, 69].

In contrast to crystalline solids, collective excitations (phonons) are unable to exist in non-crystalline solids. Above approximately 50 K, the thermal conductivity of non-crystalline solids decreases with decreasing temperatures and is well-described by Einstein's picture of a random walk of thermal energy between localized oscillators vibrating with random phases [2, 7]. Within the context of the topological framework presented in this article, this random phase assumption has its origins in the fact that the kinetic energy term in the $O(4)$ Hamiltonian favors orientational disorder in the low-temperature solid state. In the absence of potential energy effects, the solid that forms is a physical realization of a system of Einstein oscillators that are entirely uncoupled and thus cannot transmit thermal energy throughout the system. Real non-crystalline solids (green) exhibit some orientational correlations between neighboring atomic clusters, that allow for heat transfer by a random walk mechanism.

4. Summary and conclusions

Ideas advanced in this article are based on seminal work spanning a wide range of fields. These ideas offer a perspective on the topological origins of the development of solid states as well as their thermal transport properties. The topological framework presented herein has enabled the generalization of the notion of restricted dimensions among complex, and quaternion algebra domains (see table 1). In particular, we have:

- introduced a quaternion orientational order parameter for solidification, which characterizes the topological structure of undercooled atomic fluids.
- identified four- and three-dimensions as restricted dimensions for quaternion ordered systems, such that O(4) quantum rotor models apply.
- identified an important role of third homotopy group topological defects in solidification.
- presented a topological perspective on the necessity of undercooling below the melting temperature prior to the formation of the solid state.
- utilized uncertainty relations that apply to quaternion ordered systems, between amplitude and scalar phase angle parameters, to invoke a duality between crystallization and the glass transition that can be realized in restricted dimensions. This has enabled the development of a phase diagram for solidification, in analogy to the phase diagram for $O(2)$ JJAs in the vicinity of the superconductor-to-superinsulator transition.
- classified ordered major skeleton networks, induced by geometrical frustration, as a consequence of finite kinetic energy effects in $O(4)$ quantum rotor models.
- introduced a topological perspective of the well-known Kauzmann point, relating it to the 'self-dual' critical point in $O(4)$ quantum rotor models.
- compared the inverse thermal transport properties of crystalline and non-crystalline solid states, above approximately 50 K, to the inverse temperature dependence of the electrical transport properties of $O(2)$ JJAs across the superconductor-to-superinsulator transition.

Acknowledgment

The authors would like to thank Michael Widom for useful discussions on this research topic. CSG is grateful for funding from NASA's Office of Graduate Research via the Space Technology and Research Fellowship (NSTRF). We also acknowledge support from the ALCOA Chair in Physical Metallurgy.

ORCID iDs

Caroline S Gorham https://orcid.org/0000-0002-9135-1003
David E Laughlin https://orcid.org/0000-0002-9819-7897

References

[1] Kittel C 1949 Interpretation of the thermal conductivity of glasses *Phys. Rev.* **75** 972–4
[2] Cahill D G and Pohl R O 1988 Lattice vibrations and heat transport in crystals and glasses *Annu. Rev. Phys. Chem.* **39** 93–121
[3] Orbach R 1993 Phonon localization and transport in disordered systems *J. Non-Cryst. Solids* **164–6** 917–22
[4] Dove M T 1993 *Introduction to Lattice Dynamics* vol 4 (Cambridge: Cambridge University Press)
[5] Kittel C and McEuen P 1996 *Introduction to Solid State Physics* vol 7 (New York: Wiley)
[6] Eucken A 1911 Über die temperaturabhängigkeit der wärmeleitfähigkeit fester nichtmetalle *Ann. Phys.* **339** 185–221
[7] Cahill D G, Watson S K and Pohl R O 1992 Lower limit to the thermal conductivity of disordered crystals *Phys. Rev.* B **46** 6131–40
[8] Frank F C 1952 Supercooling of liquids *Proc. R. Soc.* A **215** 43–121
[9] Nelson D R 1983 Liquids and glasses in spaces of incommensurate curvature *Phys. Rev. Lett.* **50** 982–5
[10] Sethna J P, Wright D C and Mermin N D 1983 Relieving cholesteric frustration: the blue phase in a curved space *Phys. Rev. Lett.* **51** 467
[11] Nelson D R and Widom M 1984 Symmetry, Landau theory and polytope models of glass *Nucl. Phys.* B **240** 113–39
[12] Halperin B I and Nelson D R 1978 Theory of two-dimensional melting *Phys. Rev. Lett.* **41** 121
[13] Landau L D and Lifshitz E M 1986 *Theory of Elasticity, vol 7* (*Course of Theoretical Physics* vol 3)

[14] Chaikin P M and Lubensky T C 2000 *Principles of Condensed Matter Physics* vol 1 (Cambridge: Cambridge University Press)
[15] Pretko M and Radzihovsky L 2018 Fracton-elasticity duality *Phys. Rev. Lett.* **120** 195301
[16] Yazyev O V and Chen Y P 2014 Polycrystalline graphene and other two-dimensional materials *Nat. Nanotechnol.* **9** 755
[17] Kosterlitz J M and Thouless D J 1973 Ordering, metastability and phase transitions in two-dimensional systems *J. Phys. C: Solid State Phys.* **6** 1181
[18] Halperin B I and Nelson D R 1979 Resistive transition in superconducting films *J. Low Temp. Phys.* **36** 599–616
[19] Herbut I 2007 *A Modern Approach to Critical Phenomena* (Cambridge: Cambridge University Press)
[20] Poran S, Nguyen-Duc T, Auerbach A, Dupuis N, Frydman A and Bourgeois O 2017 Quantum criticality at the superconductor-insulator transition revealed by specific heat measurements *Nat. Commun.* **8** 14464
[21] Mermin N D and Wagner H 1966 Absence of ferromagnetism or antiferromagnetism in one- or two-dimensional isotropic Heisenberg models *Phys. Rev. Lett.* **17** 1133–6
[22] Berezinskii V L 1971 Destruction of long-range order in one-dimensional and two-dimensional systems having a continuous symmetry group I. Classical systems *Sov. Phys.—JETP* **32** 493–500
[23] Gorham C S and Laughlin D E 2018 SU(2) orientational ordering in restricted dimensions: evidence for a Berezinskii–Kosterlitz–Thouless transition of topological point defects in four dimensions *J. Phys. Commun.* **2** 075001
[24] Vinokur V M, Baturina T I, Fistul M V, Mironov A Y, Baklanov M R and Strunk C 2008 Superinsulator and quantum synchronization *Nature* **452** 613
[25] Sachdev S 2011 *Quantum Phase Transitions* (New York: Cambridge University Press)
[26] Vojta T and Sknepnek R 2006 Quantum phase transitions of the diluted O(3) rotor model *Phys. Rev.* B **74** 094415
[27] Gantmakher V F and Dolgopolov V T 2010 Superconductor–insulator quantum phase transition *Phys.—Usp.* **53** 1–49
[28] Baturina T I and Vinokur V M 2013 Superinsulator-superconductor duality in two dimensions *Ann. Phys.* **331** 236–57
[29] Mermin N D 1978 The homotopy groups of condensed matter physics *J. Math. Phys.* **19** 1457–62
[30] Mermin N D 1979 The topological theory of defects in ordered media *Rev. Mod. Phys.* **51** 591
[31] Nelson D R 2002 *Defects and Geometry in Condensed Matter Physics* (Cambridge: Cambridge University Press)
[32] Sadoc J-F and Mosseri R 2006 *Geometrical Frustration* (Cambridge: Cambridge University Press)
[33] Griffin S M and Spaldin N A 2017 On the relationship between topological and geometric defects *J. Phys.: Condens. Matter* **29** 343001
[34] Stillwell J 2001 The story of the 120-cell *Notices Am. Math. Soc.* **48** 17–24
[35] Toulouse G and Kléman M 1976 Principles of a classification of defects in ordered media *J. Phys. Lett.* **37** 149–51
[36] Sethna J 2006 *Statistical Mechanics, Order Parameters and Complexity* vol 14 (Oxford: Oxford University Press)
[37] Hull D and Bacon D J 2001 *Introduction to Dislocations* (Oxford: Butterworth-Heinemann)
[38] Teo J C and Kane C L 2010 Topological defects and gapless modes in insulators and superconductors *Phys. Rev.* B **82** 115120
[39] Teo J C T and Hughes T L 2017 Topological defects in symmetry-protected topological phases *Annu. Rev. Condens. Matter Phys.* **8** 211–37
[40] Nambu Y 1960 Quasi-particles and gauge invariance in the theory of superconductivity *Phys. Rev.* **117** 648–63
[41] Goldstone J, Salam A and Weinberg S 1962 Broken symmetries *Phys. Rev.* **127** 965
[42] Zhang S-C and Hu J 2001 A four-dimensional generalization of the quantum Hall effect *Science* **294** 823–8
[43] Bernevig B A, Hu J, Toumbas N and Zhang S-C 2003 Eight-dimensional quantum Hall effect and 'octonions' *Phys. Rev. Lett.* **91** 236803
[44] Ising E 1925 Beitrag zur theorie des ferromagnetismus *Z. Phys.* **31** 253–8
[45] Onsager L 1944 Crystal statistics. I. A two-dimensional model with an order-disorder transition *Phys. Rev.* **65** 117
[46] Fazio R and Schön G 2013 Charges and vortices in Josephson junction arrays *40 Years of Berezinskii–Kosterlitz–Thouless Theory* (Singapore: World Scientific) pp 237–54
[47] Kosterlitz J M 1974 The critical properties of the two-dimensional xy model *J. Phys. C: Solid State Phys.* **7** 1046
[48] Sadoc J F 1985 Orientational order in disordered systems *J. Phys. Colloques* **46** C9–79
[49] Alexander G P, Chen B G-G, Matsumoto E A and Kamien R 2012 Colloquium: disclination loops, point defects, and all that in nematic liquid crystals *Rev. Mod. Phys.* **84** 497
[50] Hatcher A 2002 *Algebraic Topology* (Cambridge: Cambridge University Press)
[51] Doye J P and Wales D J 1996 The effect of the range of the potential on the structure and stability of simple liquids: from clusters to bulk, from sodium to C60 *J. Phys. B: At. Mol. Opt. Phys.* **29** 4859
[52] Teitel S and Jayaprakash C 1983 Josephson-junction arrays in transverse magnetic fields *Phys. Rev. Lett.* **51** 1999
[53] Venkataraman G, Sahoo D and Balakrishnan V 1989 *Beyond the Crystalline State: an Emerging Perspective* vol 84 (Berlin: Springer)
[54] Romanov A E and Vladimirov V I 1983 Disclinations in solids *Phys. Status Solidi* a **78** 11–34
[55] Mosseri R 2008 Geometrical frustration and defects in condensed matter systems *C. R. Chim.* **11** 192–7
[56] Frank F C and Kasper J S 1959 Complex alloy structures regarded as sphere packings. II. Analysis and classification of representative structures *Acta Crystallogr.* **12** 483–99
[57] Frank F C and Kasper J S 1958 Complex alloy structures regarded as sphere packings. I. Definitions and basic principles *Acta Crystallogr.* **11** 184–90
[58] De Graef M and McHenry M E 2012 *Structure of Materials: an Introduction to Crystallography, Diffraction and Symmetry* (Cambridge: Cambridge University Press)
[59] Angell C A 1990 Relaxation, glass formation, nucleation, & rupture in normal and 'water-like' liquids at low temperatures and/or negative pressures *Correlations and Connectivity* (Berlin: Springer) pp 133–60
[60] Mooij J E, van Wees B J, Geerligs L J, Peters M, Fazio R and Schön G 1990 Unbinding of charge-anticharge pairs in two-dimensional arrays of small tunnel junctions *Phys. Rev. Lett.* **65** 645
[61] Langer J 2007 The mysterious glass transition *Phys. Today* **60** 8
[62] Kauzmann W 1948 The nature of the glassy state and the behavior of liquids at low temperatures *Chem. Rev.* **43** 219–56
[63] Stillinger F H 1988 Supercooled liquids, glass transitions, and the Kauzmann paradox *J. Chem. Phys.* **88** 7818–25
[64] Stillinger F H, Debenedetti P G and Truskett T M 2001 The Kauzmann paradox revisited *J. Phys. Chem.* B **105** 11809–16
[65] Debenedetti P G and Stillinger F H 2001 Supercooled liquids and the glass transition *Nature* **410** 259

[66] Speedy R J 2003 Kauzmann's paradox and the glass transition *Biophys. Chem.* **105** 411–20
[67] Debenedetti P G, Truskett T M, Lewis C P and Stillinger F H 2001 Theory of supercooled liquids and glasses: energy landscape and statistical geometry perspectives *Adv. Chem. Eng.* **28** 21–79
[68] Michalski J and Erdös P 1989 Comparison of the thermal properties of two-dimensional periodic and aperiodic lattice models *Solid State Commun.* **72** 967–70
[69] Michalski J 1992 Thermal conductivity of amorphous solids above the plateau: molecular-dynamics study *Phys. Rev.* B **45** 7054